# Graphene/$SiO_2$/p-GaN Diodes: An Advanced Economical Alternative for Electrically Tunable Light Emitters

*Che-Wei Chang, Wei-Chun Tan, Meng-Lin Lu, Tai-Chun Pan, Ying-Jay Yang, and Yang-Fang Chen**

**Advanced materials that combine novel functionality and ease of applicability are central to the development of light-emitting diodes (LEDs), which is of ever increasing commercial importance. Here a new metal-insulator-semiconductor (MIS) LED structure that combines economical fabrication with novel device properties is reported. The presented MIS-LED consists of a graphene electrode on p-GaN substrate separated by an insulating $SiO_2$ layer. It is found that the MIS-LED possesses a unique tunability of the electroluminescence spectra depending on the bias conditions. Tunnel injection from graphene into the p-GaN can explain the difference in luminescence spectra under forward and reverse bias. The demonstrated MIS-LED expands the use of graphene and also possibly allows the direct integration of light emitters with other circuit elements.**

## 1. Introduction

The technology of electrically generated light plays a vital role in our daily life, including illumination, display panels and traffic signals, and accounts to approximately 20% of the global energy consumption. Due to their high efficiency, LEDs could help decrease power consumption on a global scale. However, in order to maximize their commercial impact, improvements in the cost efficiency of LEDs are required. Group III-nitride semiconductors have been a focus for optoelectronics devices due to their composition dependent variable bandgap. InGaN based LEDs and laser diodes, for example, can cover the spectrum from UV to visible light.[1–7] Although group III-nitrides are well researched, there still exists difficulty in emitting different colors from a single chip for integrated optoelectronics. Fortunately, recent works based on GaN and ZnO demonstrated the electrically tunable electroluminescence (EL) from nanostructures and semiconductor-insulator-semiconductor (SIS) structures.[8–11] These reports have stirred up considerable interest in electrically tunable LEDs. However, electrically tunable LEDs based on metal-insulator-semiconductor (MIS) devices have not been reported thus far. MIS-LEDs, in contrast to conventional LEDs and SIS-LEDs, are attractive for several reasons. First of all, MIS-LEDs do not require complex process involving multiple-quantum-wells (MQWs) and nanostructures. Moreover, MIS-LEDs do not rely p-n junctions, which expand the list of usable semiconductors to materials that cannot be easily doped. However, MIS-LEDs require metal electrodes with high transparency, which poses severe limitations.

Recently, the use of graphene as a transparent metal contact to optoelectronic devices has been intensively investigated.[12–14] Graphene, an atomically thin film composed of a single layer of carbon, has attracted significant attention due to its exceptionally electrical and optical properties.[15–20] In contrast to indium tin oxide (ITO), graphene possesses high electron and hole mobility, high transparency and high robustness. Therefore, graphene has been considered a promising conducting material offering low cost and high transparency in comparison with other frequently used conducting materials, such as Ni/Au and ITO. Stimulated by these attractive features, we fabricated MIS-LEDs using graphene layer as a metal contact on p-GaN substrate with an insulating $SiO_2$ interlayer. The newly designed MIS-LEDs can be easily and economically fabricated and exhibit tunable electroluminescence spectra under forward or reverse bias polarities at room temperature. A near band-edge (UV) light emission is observed under forward bias and a defect-related (orange-red) light emission is observed under reverse bias. The underlying mechanism can be understood in terms of carrier tunneling through the thin oxide layer in both bias polarities, which is different from the standard p-n junction model. Notably, the creation of MIS-LEDs can expand the practical applications of LEDs because it is capable of overcoming the difficulty in the integration of light emitters, transistors and

C.-W. Chang, W.-C. Tan, M.-L. Lu, Prof. Y.-F. Chen
Department of Physics
National Taiwan University
No. 1, Sec. 4, Roosevelt Road, Taipei 106,
Taiwan, Republic of China
E-mail: yfchen@phys.ntu.edu.tw
T.-C. Pan
Institute of Optoelectronic Sciences
National Taiwan Ocean University
No.2, Pei-Ning Road, Keelung 224, Taiwan, Republic of China
C.-W. Chang, Prof. Y.-J. Yang
Graduate Institute of Electronics Engineering
National Taiwan University
No. 1, Sec. 4, Roosevelt Road, Taipei 106, Taiwan, Republic of China
Prof. Y.-F. Chen
Center for Emerging Material and Advanced Devices
National Taiwan University
No. 1, Sec. 4, Roosevelt Road, Taipei 106, Taiwan, Republic of China

**DOI: 10.1002/adfm.201203035**

memories. Our work therefore not only demonstrates a new application of the 2D graphene crystal, but also opens up a new class of optoelectronic devices.

## 2. Results and Discussion

Graphene was synthesized by chemical vapor deposition as described previously.[21] The thickness and quality of the prepared graphene can be evaluated from the Raman spectra shown in **Figure 1**a. The intensity ratio between 2D and G bands reveals that our graphene is single layer or bilayer. The homogeneous deposition of graphene on $SiO_2$ can be inferred from atomic force microscopy (AFM) images as shown in the inset of Figure 1a. Figure 1b shows the transmittance of the graphene in comparison to Au thin films of different thicknesses in the wavelength range from 400 nm to 1100 nm. In contrast to Au thin films, the high transmittance and wide transmission range make graphene well suited as a transparent electrode. Additionally, the quality of graphene was investigated through electrical transport measurements. For this purpose, a field-effect device was made from graphene/$SiO_2$/p-Si in a back-gate transistor structure. Figure 1c shows the back-gate transfer characteristics under a low source-drain bias (10 mV). The field-effect carrier mobility can be extracted from the linear regime[22]

$$\mu = \frac{L g_m}{W C_{ox} V_{ds}} \quad (1)$$

where $L$ and $W$ are the channel length and the channel width, $g_m$ is the transconductance, $C_{ox}$ is the oxide capacitance, and $V_{ds}$ is the channel bias. It is found that the field-effect carrier mobility of the CVD graphene used is about 1100 $cm^2\ v^{-1}\ s^{-1}$.

The graphene was used to fabricate MIS-LEDs in the configuration shown in **Figure 2**a. Here, the large-area CVD graphene was used as a cathode and a Ni/Au contact was used as the anode. The presence of graphene in the fabricated device was confirmed by AFM images after processing as shown in the inset of Figure 2a. The thickness of the $SiO_2$ tunneling barrier was approximately 10 nm. The quality of the p-GaN substrate was investigated by photoluminescence (PL) spectroscopy under light excitation of 325 nm at room temperature (Figure 2b). The PL spectrum is dominated by a blue emission peak at ≈415 nm and a broadband yellow emission at ≈550 nm. The emission peak at ≈415 nm can be attributed to the transition from the energy level 170 meV below the conduction band originating from interstitial Mg atoms to the energy level 250 meV above the valence band due to acceptor impurities.[23] These doping-related energy levels strongly depend on the carrier density, that is, increase of the doping concentration results in the dominance of blue and yellow emission in the PL spectra.[24] Moreover, it has been reported that the intensity of the blue emission is not only related to the doping concentration, but also depends on the crystalline structure of p-GaN.[24,25] In contrast to the blue emission, the yellow emission centered at ≈550 nm could be attributed to the dislocations of atoms or native point defects.[25] Our observation that the yellow emission changes during the ohmic contact formation step of the device fabrication process can be interpreted as annealing induced changes in the point defect concentration of p-GaN.[25,26].

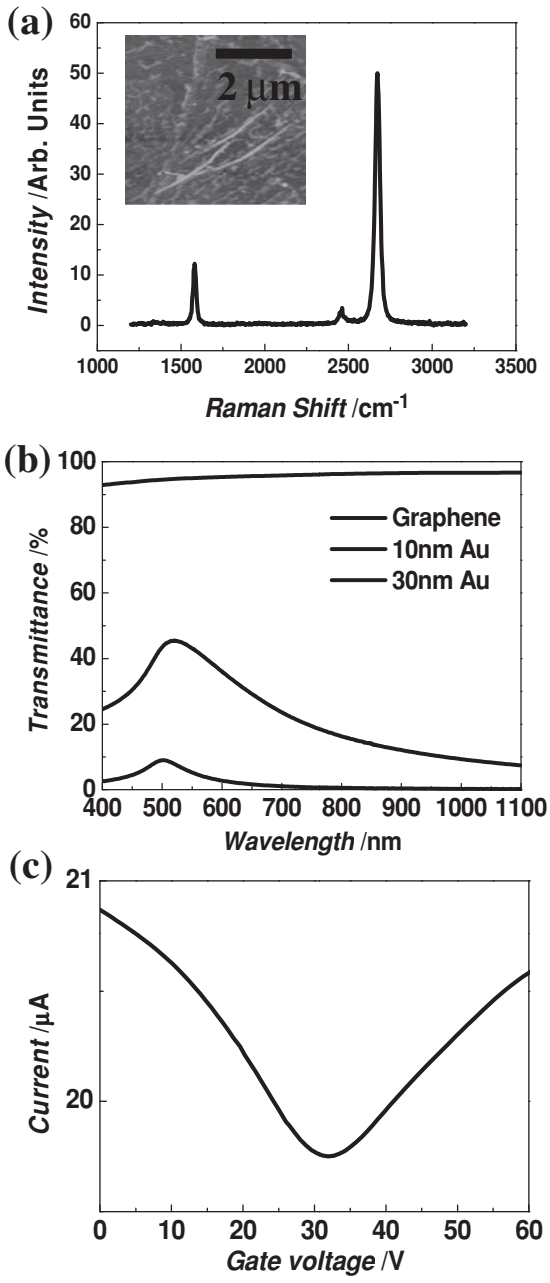


**Figure 1.** a) Raman spectrum and atomic force microscope (AFM) image (inset) of a graphene layer transferred onto $SiO_2$. b) Optical transmission spectra of graphene compared to Au thin films. c) Back-gate transfer characteristics of a graphene field-effect transistor.

**Figure 3**a shows the EL spectra of the produced MIS-LED under forward bias with different injection currents at room temperature. At moderate injection currents, the MIS-LEDs exhibit mostly UV emission originating from the near-band-edge emission. One of the most important observations of our experiments is that the MIS devices also show EL signal under reverse bias at low injection currents, as shown in Figure 3b. It can be seen that, in contrast to the forward bias condition, the orange-red emission dominates the spectra and UV emission appears only at higher injection current under reverse bias. The

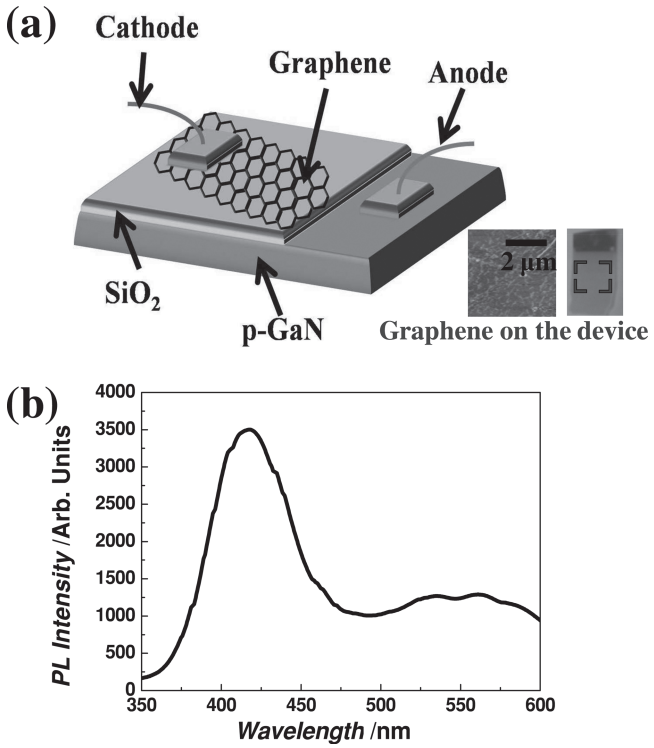


**Figure 2.** a) Schematics of graphene/$SiO_2$/p-GaN MIS-LED and AFM image (inset) of the graphene electrode and photograph of the device. b) Photoluminescence spectrum of p-GaN at room temperature.

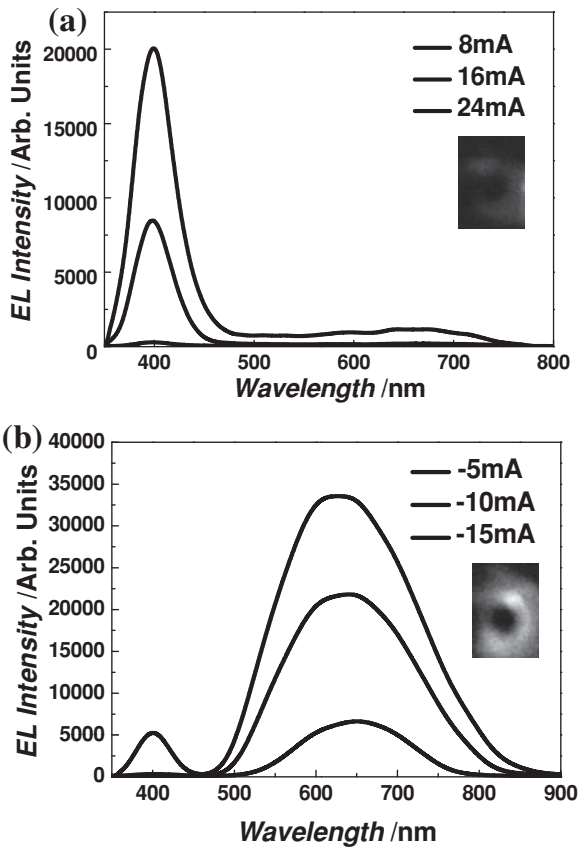


**Figure 3.** a) EL spectra of graphene/$SiO_2$/p-GaN MIS-LEDs under forward bias at different injection currents at room temperature. The inset shows a photograph of the light emission from MIS-LEDs under forward bias. b) EL spectra of graphene/$SiO_2$/p-GaN MIS-LEDs under reverse bias at different injection currents at room temperature. The inset shows a photograph of the light emission from MIS-LEDs under reverse bias.

photographs of the light emission from a MIS-LED under both bias polarities are shown in the inset of Figure 3 indicating the strong emission arising from the device at room temperature.

The observed light-emission of the MIS-LEDs cannot be explained by the light-emitting mechanism of p-n junction LEDs. The light emission of reverse biased p-n junctions is commonly interpreted in terms of the recombination of carriers created by impact ionization, which is characterized by a broad-band emission.[27,28] Impact ionization, however, is not applicable to our MIS-LED since avalanche multiplication should be most efficient at high injection currents under reverse bias. This prediction is in stark contrast with our experimental observation that the injection current of the MIS-LED under reverse bias is smaller than under forward bias, as shown in Figure 3a,b. Furthermore, our MIS device structure is very different from p-n junctions, since a thin $SiO_2$ layer was grown as a tunneling barrier between graphene and p-GaN. Therefore, the light emission is expected to result from the radiative combination of carriers injected from graphene which tunnel through the $SiO_2$ layer.

In order to understand the underlying mechanism of the observed EL spectra under forward and reverse biases, we examined the band structure of our device. **Figure 4**a shows a schematic view of the MIS-LED band diagram under thermal equilibrium following previous reports.[29–31] Under forward bias (negative bias applied on graphene), shown in Figure 4b, the bands of p-GaN near the $SiO_2$ layer are bent upward and the Fermi level of graphene moves upward. Therefore, tunnel injection of electrons from graphene into the conduction band of p-GaN occurs. Due to the insulating $SiO_2$ layer as an energy barrier, the applied electric-field induces an accumulation layer of holes at the p-GaN/$SiO_2$ interface. The injected electrons recombine radiatively with the holes in the acceptor levels of p-GaN and generate the UV emission. The weak orange-red emission observed in Figure 3a can be understood by the recombination of tunnel electrons from the conduction band to holes in the deep acceptor levels.[32] The difference in the peak position of our work (orange-red) and previous reports on deep acceptor level recombination (yellow) could originate from different band alignment across the $SiO_2$ layer induced by the different materials used in our experiments.[32]

Similarly, under reverse bias the EL spectra stem from the injection of holes from graphene into p-GaN. In this case, the bands of p-GaN near the $SiO_2$ are bent downward. At the same time, the Fermi level of graphene moves downward. Due to the insulating $SiO_2$ layer as an energy barrier, the applied electric-field induces an inversion layer at the p-GaN/$SiO_2$ interface and accumulation of electrons occurs, as shown in Figure 4c. Injection of holes from graphene into the acceptor level of p-GaN is attributed to tunneling under reverse bias. The orange-red emission observed in Figure 3b can be understood

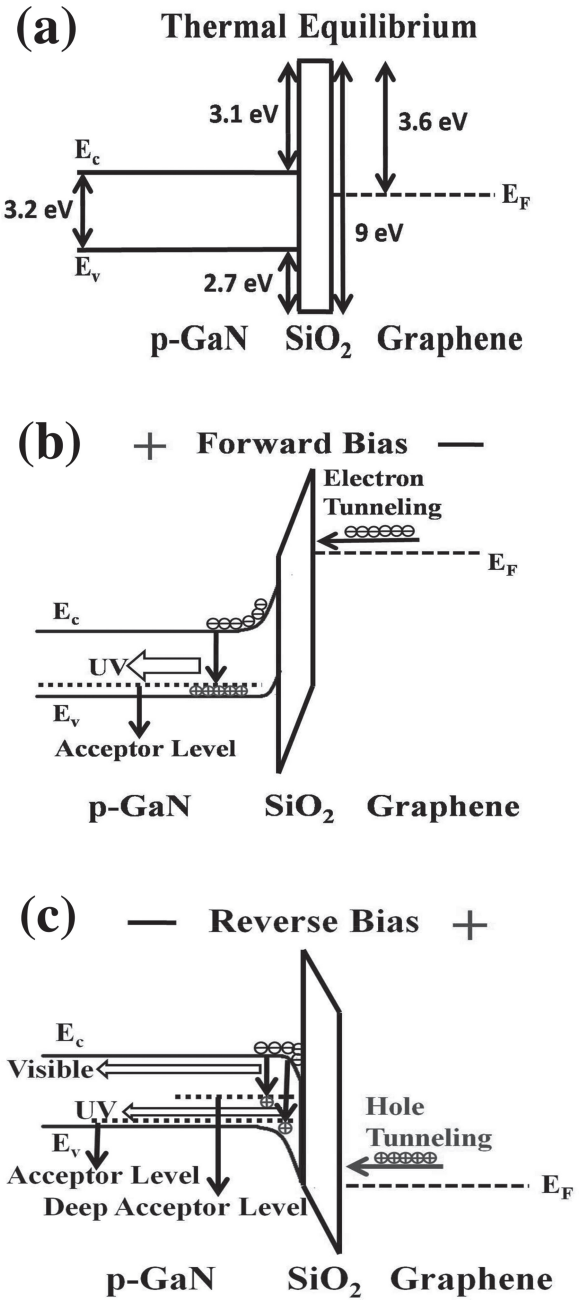


**Figure 4.** a) Energy band diagram of graphene/$SiO_2$/p-GaN MIS-LEDs under thermal equilibrium. b) Energy band diagram of graphene/$SiO_2$/p-GaN MIS-LEDs under forward bias. c) Energy band diagram of graphene/$SiO_2$/p-GaN MIS-LEDs under reverse bias.

by the recombination of tunnel holes from the deep acceptor level with electrons in the conduction band. The recombination process of UV emission can be attributed to the transition from the conduction band of p-GaN to the acceptor level when the external bias is high enough.

To further confirm our proposed tunneling model, we quantitatively analyze the relationship between the integrated intensity $I$ of the EL spectra and the applied bias V. According to

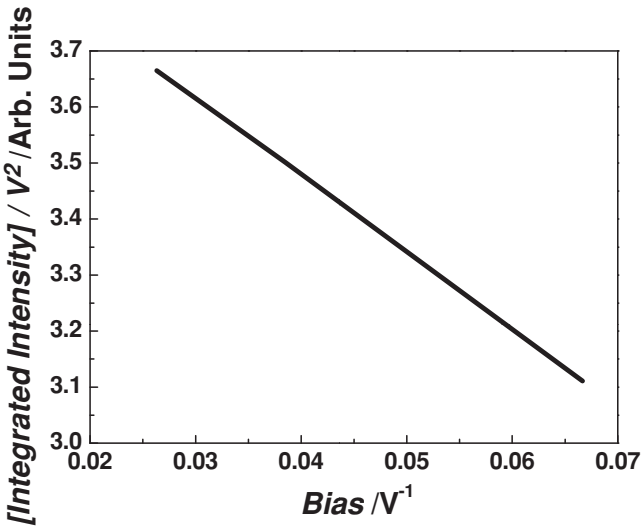


**Figure 5.** Integrated electroluminescence intensity of graphene/$SiO_2$/p-GaN MIS-LEDs, divided by $V^2$, as a function of $V^{-1}$ under reverse bias.

previous reports,[33,34] within the Simmon's approximation, in the limit of large applied bias, the dependence of $I$ versus $V$ can be written as,

$$I \propto V^2 \exp\left(-\frac{4d\sqrt{2m_e\phi^3}}{3\hbar e V}\right) \quad (2)$$

where $d$ is the barrier width, $m_e$ is the electron effective mass, and $\phi$ is the tunnel barrier height. **Figure 5** shows the integrated intensity divided by $V^2$ as a function of $V^{-1}$ under reverse bias, and a linear dependence is obtained. Therefore, our result demonstrates that carrier tunneling is the dominant emission mechanism in our MIS-LEDs.

In order to demonstrate the impact of graphene electrodes on the performance of MIS-LEDs, we also fabricated and characterized the MIS-LEDs with Au thin film electrodes. It is found that the light emission of MIS-LED devices with Au thin film thicker than 30 nm can hardly be detected. This result can be easily understood by recalling the difference in transmittance spectra between graphene and Au shown in Figure 1b. For Au thin films with a thickness of 10 nm, the MIS-LED device is able to generate light emission under both forward and reverse biases as shown in **Figure 6**a,b, respectively. However, the light intensity is much smaller than that of the device made with graphene. Consequently, the excellent optical and electrical properties and potential low cost fabrication make graphene a superior electrode material for the creation of MIS-LED devices.

Finally, the important role played by the $SiO_2$ tunneling barrier is worth mentioning. Without the insulating layer, the EL signal is very weak or even negligible (not shown here). This is due to the double role of the $SiO_2$ layer to prevent the occurrence of leakage current and to accumulate free carriers near the interface as shown in Figure 4. We therefore anticipate that further optimization of the $SiO_2$ layer thickness and quality can be used to enhance the EL intensity even more.

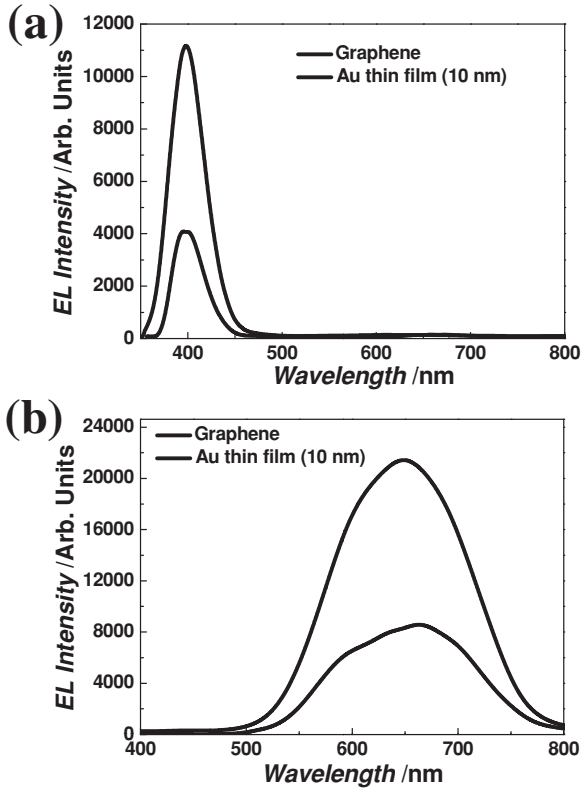


**Figure 6.** a) Comparison of electroluminescence spectra from graphene/$SiO_2$/p-GaN MIS-LEDs and Au/$SiO_2$/p-GaN MIS-LEDs under forward bias. b) Comparison of electroluminescence spectra from graphene/$SiO_2$/p-GaN MIS-LEDs and Au/$SiO_2$/p-GaN MIS-LEDs under reverse bias.

## 3. Conclusion

In summary, we have developed a new MIS-LED with tunable emission spectra when used under forward and reverse biases. The high performance of our MIS-LED is made possible by taking advantage of the excellent transparency and conductivity of graphene. The observed EL spectra under both forward and reverse biases can be interpreted by the tunneling of electrons and holes through the insulating layer, respectively. This approach may aid in the development of economical alternatives to current tunable LEDs and represents a novel application of graphene in MIS-based optoelectronic devices. In addition, the use of graphene as a versatile electrode could enable the integration of transistors and memory devices into the presented MIS structures and open up a new area of research.

## 4. Experimental Section

*Device Fabrication*: p-type, Mg doped GaN with doping levels of $3 \times 10^{17}$ $cm^{-3}$ was used as the substrate. First, a p-GaN wafer was rinsed in acetone, isopropyl alcohol, and DI water. To obtain a low resistance ohmic contact on p-GaN, Ni/Au was annealed after deposition following previous report.[35] Insulating $SiO_2$ layers were deposited on p-GaN via RF sputtering after the formation of Ni/Au ohmic contact. Graphene was grown on copper foils at temperature of 1000 °C following a previously reported CVD process.[21] Polymethyl-methacrylate (PMMA) was used to transfer and align graphene onto the p-GaN.

## Acknowledgements

This work was supported by the National Science Council and Ministry of Education of the Republic of China.

Received: October 17, 2012
Revised: December 27, 2012
Published online: March 11, 2013

[1] S. Nakamura, M. Senoh, T. Mukai, *Appl. Phys. Lett.* **1993**, *62*, 2390.
[2] I. Akasaki, S. Sota, H. Sakai, T. Tanaka, M. Koike, H. Amano, *Electron. Lett.* **1996**, *32*, 1105.
[3] P. Waltereit, O. Brandt, A. Trampert, H. T. Grahn, J. Menniger, M. Ramsteiner, M. Reiche, K. H. Ploog, *Nature* **2000**, *406*, 865.
[4] H. M. Kim, T. W. Kang, K. S. Chung, *Adv. Mater.* **2003**, *15*, 567.
[5] J. J. Wierer, M. R. Krames, J. E. Epler, N. F. Gardner, M. G. Craford, J. R. Wendt, J. A. Simmons, M. M. Sigalas, *Appl. Phys. Lett.* **2004**, *84*, 3885.
[6] N. F. Gardner, G. O. Müller, Y. C. Shen, G. Chen, S. Watanabe, W. Götz, M. R. Krames, *Appl. Phys. Lett.* **2007**, *91*, 243506.
[7] M. K. Kwon, J. Y. Kim, B. H. Kim, I. K. Park, C. Y. Cho, C. C. Byeon, S. J. Park, *Adv. Mater.* **2008**, *20*, 1253.
[8] M. A. Zimmler, J. M. Bao, I. Shalish, W. Yi, J. Yoon, V. Narayanamurti, F. Capasso, *Nanotechnology* **2007**, *18*, 235205.
[9] H. K. Fu, C. L. Cheng, C. H. Wang, T. Y. Lin, Y. F. Chen, *Adv. Funct. Mater.* **2009**, *19*, 3471.
[10] Y. J. Hong, C. H. Lee, A. Yoon, M. Y. Kim, H. K. Seong, H. J. Chung, Ch. Sone, Y. J. Park, G. C. Yi, *Adv. Mater.* **2011**, *23*, 3284.
[11] X. Y. Chen, A. M. C. Ng, F. Fang, Y. H. Ng, A. B. Djurišić, H. L. Tam, K. W. Cheah, S. Gwo, W. K. Chan, H. F. Lui, P. W. K. Fong, C. Surya, *J. Appl. Phys.* **2011**, *110*, 094513.
[12] W. W. Cai, Y. W. Zhu, X. S. Li, R. D. Piner, R. S. Ruoff, *Appl. Phys. Lett.* **2009**, *95*, 123115.
[13] X. Li, H. Zhu, K. Wang, A. Cao, J. Wei, C. Li, Yi Jia, Z. Li, X. Li, D. Wu, *Adv. Mater.* **2010**, *22*, 2743.
[14] S. Chandramohan, J. H. Kang, Y. S. Katharria, N. Han, Y. S. Beak, K. B. Ko, J. B. Park, H. K. Kim, E. K. Suh, C. H. Hong, *Appl. Phys. Lett.* **2012**, *100*, 023502.
[15] K. S. Novoselov, A. K. Geim, S. V. Morozov, D. Jiang, Y. Zhang, S. V. Dubonos, I. V. Grigorieva, A. A. Firsov, *Science* **2004**, *306*, 666.
[16] A. K. Geim, K. S. Novoselov, *Nat. Mater.* **2007**, *6*, 183.
[17] Y. Zhang, Y. W. Tan, H. L. Stormer, P. Kim, *Nature* **2005**, *438*, 201.
[18] C. Berger, Z. Song, X. Li, X. Wu, N. Brown, C. Naud, D. Mayou, T. Li, J. Hass, A. N. Marchenkov, E. H. Conrad, P. N. First, W. A. de Heer, *Science* **2006**, *312*, 1191.
[19] D. A. Areshkin, C. T. White, *Nano Lett.* **2007**, *7*, 3253.
[20] V. Ryzhii, M. Ryzhii, A. Satou, T. Otsuji, A. A.Dubinov, V. Ya. Aleshkin, *J. Appl. Phys.* **2009**, *106*, 084507.
[21] W.C. Tan, M. Hofmann, Y.P. Hsieh, M.L. Lu, Y.F. Chen, *Nano Res.* **2012**, *5*, 695
[22] O. M. Nayfeh, *IEEE Trans. Electron Devices* **2011**, *58*, 2847.
[23] M. Smith, G. D. Chen, J. Y. Lin, H. X. Jiang, A. Salvador, B. N. Sverdlov, A. Botchkarev, H. Morkoc, B. Goldenberg, *Appl. Phys. Lett.* **1996**, *68*, 1883.
[24] C. Guarneros, V. Sánchez, *Mater. Sci. Eng. B* **2010**, *174*, 263.
[25] S.Y. Xie, Y.D. Zheng, P. Chen, R. Zhang, B. Shen, H. Chen, *Appl. Phys. A* **2002**, *75*, 363.

[26] B.J. Pong, C.J. Pan, Y.C. Teng, C.G. Chi, W.H. Li, K.C. Lee, C.H. Lee, *J. Appl. Phys.* **1998**, *83*, 5992.
[27] Y. I. Alivov, D. C. Look, B. M. Ataev, M. V. Chukichev, V. V. Mamedov, V. I. Zinenko, Y. A. Agafonov, A. N. Pustovit, *Solid-State Electron.* **2004**, *48*, 2343.
[28] D. K. Hwang, M. S. Oh, J. H. Lim, Y. S. Choi, S. J. Park, *Appl. Phys. Lett.* **2007**, *91*, 121113.
[29] Z. A. Weinberg, G. W. Rubloff, E. Bassous, *Phys. Rev. B* **1979**, *19*, 3107.
[30] I. Vurgaftman, J. R. Meyer, L. R. Ram-Mohan, *J. Appl. Phys.* **2001**, *89*, 5815.
[31] Y. Yu, Y. Zhao, S. Ryu, L. E. Brus, K. S. Kim, P. Kim, *Nano Lett.* **2009**, *9*, 3430.
[32] X. Y. Chen, A. M. C. Ng, F. Fang, Y. H. Ng, A. B. Djurišić, H. L. Tam, K. W. Cheah, S. Gwo, W. K. Chan, H. F. Lui, P. W. K. Fong, C. Surya, *J. Appl. Phys.* **2011**, *110*, 094513.
[33] M. Depas, B. Vermeire, P. W. Mertens, R. L. Van Meirhaeghe, M. M. Henys, *Solid-State Electron.* **1995**, *38*, 1465.
[34] J. G. Simmons, *J. Appl. Phys.* **1963**, *34*, 1793.
[35] Q. Qiao, L. S. Yu, S. S. Lau, J. Y. Lin, H. X. Jiang, T. E. Haynes, *J. Appl. Phys.* **2000**, *88*, 4196.